Materials Science, Vol. 42, No. 2, 2006

EFFECT OF RESIDUAL STRESS-STRAIN PROFILES ON HYDROGEN-INDUCED FRACTURE OF PRESTRESSING STEEL WIRES

J. Toribio [1] **and V. Kharin** [2]

We analyze the influence of the distributions of residual stresses and strains formed after the surface treatment of cold-drawn steel wires used as the reinforcement of prestressed reinforced concrete on the susceptibility of these wires to hydrogen embrittlement characterized by the time to fracture in the tests carried out according to the regulations of the FIP (Fédération Internationale de la Précontrainte). A computational model is proposed for the prediction of the durability of wires in corrosive hydrogenated media. In the model, the accumulation of hydrogen in potential sites of fracture as a result of diffusion under the influence of stresses and plastic strains is analyzed and a criterion of critical concentration of hydrogen specifying the time of local fracture depending on the stress–strain state is formulated. The enables us to predict the influence of specific features of the distributions of residual stresses and plastic strains after various types of thermal treatment on the durability of wires under the conditions of hydrogen embrittlement.

Introduction

Prestressing of concrete structures by means of steel wires offers a powerful civil-engineering technique aimed at introducing desirable stresses and counterbalancing undesirable stresses so that the prestressing and service loading would produce stresses within specified limits [1]. Prestressing wires are usually made of eutectoid pearlitic steel heavily cold drawn to create elevated tensile properties. These wires, once subjected to high service stresses, remain in this state forever, usually in hostile environments, e.g., due to atmospheric humidity. All these features make them sensible to the presence of surface cracks, in particular, those of stress corrosion origin. Stress corrosion cracking of prestressing steel wires was a subject of extensive studies, which substantiated the important role of hydrogen-induced fracture (HIF) or hydrogen-assisted cracking in the deterioration of reinforced-concrete structures [2]. To evaluate the susceptibility of prestressing steels to stress-corrosion cracking in general, and to HIF in particular, the International Federation for Prestressing [FIP (Fédération Internationale de la Précontrainte)] adopted the use of the ammonium-thiocyanate test (ATT) for checking steels [3]. However, despite being in use as a standard test method, it reveals neither how HIF goes in prestressing steel wires nor the roles of various manufacturing and service factors. To this end, new contributions to the better interpretation of the ATT and understanding of the process of hydrogen embrittlement in prestressing steel are welcome to gain the capability of monitoring and improving the performance of wires in hostile environments.

Residual stresses introduced by various manufacturing operations (machining, joining, and heat treating) and surface treatments (rolling, shot-peening, etc.) are known to be capable of affecting the strength and life of the components [4]. With regard to the HIF of prestressing steel wires, the importance of residual stresses produced by the rolling process was demonstrated in terms of the lives of wires in the ATT solution [5]. In the case of HIF, the role of the residual stresses is potentially twofold. First, their mechanical effect associated with the

[1] University of Salamanca, Spain.

[2] IPPMM, Ukraine.

Published in Fizyko-Khimichna Mekhanika Materialiv, Vol. 42, No. 2, pp. 105–112, March–April, 2006. Original article submitted November 11, 2005.

magnitude of residual stresses is additive to the stresses caused by applied loading [4]. In addition, the heterogeneous fields of residual stresses affect the rate of hydrogen transportation toward potential rupture sites in the wire by the stress-assisted diffusion governed by the *gradient* of the hydrostatic component of stresses [6]. Moreover, in view of the facts that residual stresses are produced by inhomogeneous plastic deformation [4] and that the indicated deformation also affects hydrogen diffusion in deformed metals [7–9], the nonuniform plastic strains caused by surface treatments should also be taken into account as factors affecting the susceptibility of wires to HIF.

The previous research [6] established an important milestone providing quantitative relationship between the *level* of residual stress (represented by some *hypothetical* residual stress distributions) and the fracture behavior of prestressing steel wires under the conditions of HIF. However, the detailed analysis of the influence of *realistic* residual stress and plastic strain profiles caused by different modes of surface rolling on the HIF susceptibility of cold-drawn prestressing steel wires has not been performed yet. In the present work, we go further in the analysis, so that the earlier developed model [6] is advanced and applied to study the influence of residual stress-and-strain distributions, e.g., similar to those formed after surface rolling, on the susceptibility of cold-drawn prestressing steel wires to hydrogen embrittlement in FIP tests.

Background Theory

In general, HIF depends on the amount of hydrogen in potential microstructural fracture sites in the metal so that the local events of rupture are associated with critical combinations of the responsible characteristics of the stress–strain field and hydrogen concentration C over a relevant material scale x_c (cell, "grain", or domain of interest), as described in [7–9]. HIF advances by the hydrogen-assisted nucleation of a (micro)crack in the site with the locally worst concentration–stress–strain triple, which can be resolved to specify the critical concentration of hydrogen C_{cr} as follows:

$$C_{\mathrm{cr}} = C_{\mathrm{cr}}(\sigma_i, \varepsilon_{pi}), \tag{1}$$

where $\sigma_i = \sigma_i(\boldsymbol{x})$ and $\varepsilon_{pi} = \varepsilon_{pi}(x)$ are, respectively, the three principal components of stresses and plastic strains $(i = 1, 2, 3)$ at the material point identified by a radius vector $\boldsymbol{x}$, which finally gives $C_{\mathrm{cr}} = C_{\mathrm{cr}}(\boldsymbol{x})$. In the particular cases of predominantly stress- or strain-controlled HIF, C_{cr} is related to the corresponding single governing mechanical variable.

Hydrogen penetrates from the corrosive environment into the metal and is accumulated in potential fracture sites until, in the course of evolution, its concentration $C(\boldsymbol{x}, t)$, where t is time, attains the critical level C_{cr} after a certain period of time t_f corresponding to the event of rupture. Then the criterion used to determine the fracture time t_f takes the form

$$C_{\mathrm{cr}}(\boldsymbol{x}_i, t_f) = C_{\mathrm{cr}}(\boldsymbol{x}_c), \tag{2}$$

where a definite fracture locus $\boldsymbol{x}_c$ must be specified.

Although hydrogen transportation toward potential damage sites comprises several consecutive stages [6–9], hydrogen diffusion in the metal is often the slowest one that controls fracture time. In particular, this is the case under the conditions of electrochemical hydrogenation, e.g., during the ATT [6, 7]. Diffusion in metals proceeds toward the maximum entropy of the system, which corresponds to the uniform distribution of a given amount of substance (represented by its concentration C) over the available occupation sites whose density can

be characterized by the solubility factor K_S. This factor depends on the dilatation of the metal lattice induced by the hydrostatic stress σ and on the amount of lattice imperfections (traps for hydrogen, cf. Hirth [10]) depending on the equivalent plastic strain ε_p, which may be expressed as follows [7–9]:

$$K_S = K_{S\varepsilon}(\varepsilon_p)\exp(\Omega\sigma) \quad \text{with} \quad \Omega = \frac{V_H}{RT}, \tag{3}$$

where $K_{S\varepsilon}$ is the strain-dependent component of solubility, V_H is the partial molar volume of hydrogen in the metal, R is the universal gas constant, and T is absolute temperature. This leads to the stress–strain affected diffusion flux [7–9]:

$$\boldsymbol{J} = -D(\varepsilon_p)\left[\nabla C - C\left(\Omega\nabla\sigma + \frac{\nabla K_{S\varepsilon}(\varepsilon_p)}{K_{S\varepsilon}(\varepsilon_p)}\right)\right], \tag{4}$$

where $D = D(\varepsilon_p)$ is the diffusion coefficient of hydrogen in the metal which characterises its mobility and depends, among other factors, on the density of lattice traps and, hence, on ε_p. The mass balance then gives the diffusion equation in terms of concentration in the form:

$$\frac{\partial C}{\partial t} = -\operatorname{div}\boldsymbol{J}. \tag{5}$$

Hydrogen entry into the metal, i.e., the boundary condition for diffusion consistent with the role of diffusion as the rate-controlling step [7–9] and with the expression for solubility (3), corresponds to the equilibrium between its environmental thermodynamic activity and concentration inside the metal on the entry surface Γ:

$$C(\Gamma, t) = C_\Gamma, \qquad C_\Gamma = C_e K_{S\varepsilon}\big(\varepsilon_p(\Gamma)\big)\exp\big(\Omega\sigma(\Gamma)\big), \tag{6}$$

where C_e is the equilibrium concentration of hydrogen in a virgin material (stress- and strain-free) under given environmental conditions. Hence, C_e stands here as a measure of the environmental thermodynamic activity of hydrogen, i.e., as the characteristic of hydrogenation capacity of the environment.

Analysis of HIF in Prestressing Wires

Description of the Test. According to the FIP proposal [3], the ATT for the evaluation of hydrogen susceptibility of prestressing steels is performed by sustained loading of smooth round wires submerged in a 20-wt.% aqueous solution of ammonium thiocyanate (NH_4SCN) and monitoring the time to fracture t_f vs. the applied axial stress σ_{ap}.

The tests [5, 6] considered in the present work were performed with prestressing steel wires of eutectoid high-strength steel cold drawn from a rod of initial diameter $d_0 = 12$ mm to get a wire of diameter $d = 7$ mm and then submitted to stress-relieve heat treatment with cooling in oil. The 0.2%-offset yield stress of a wire was $\sigma_{0.2} = 1435$ MPa and its fracture toughness in an inert environment $K_{IC} = 98\ \text{MPa}\sqrt{\text{m}}$ [5, 6]. A series of samples was tested in the as-received condition (specimens C0). The other samples were subjected to surface treatment by the rolling process under loads of 80 and 260 N (specimens C8 and C26, respectively), cf. [5].

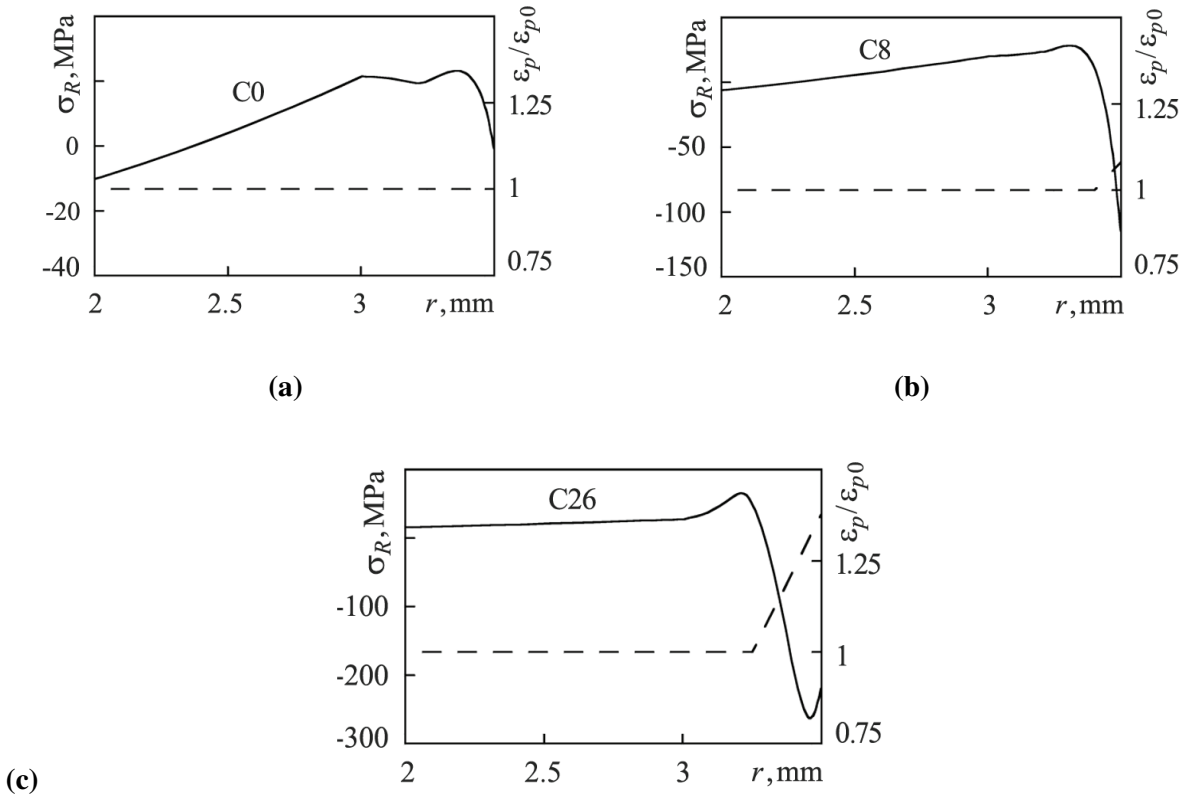

Fig. 1. Profiles of the residual hydrostatic stress (solid lines) and equivalent plastic strain (dashed lines) in cold-drawn wires C0 (a), C8 (6), and C26 (c).

Distributions of Residual Stresses and Strains. To analyze the role of surface treatments on the susceptibility of wires to hydrogen embrittlement, we used the data of X-ray diffraction measurements of the inhomogeneity of residual stresses and plastic strains [5]. These results are available for the depths from the specimen surface down to $500\,\mu\text{m}$ and mostly for the sole axial component σ_{zR} of the residual stresses. At the same time, the analysis of hydrogen diffusion requires the distributions of hydrostatic stresses over the entire radius of the wire along the radial coordinate r (for $0 \le r \le a = d/2$, where a is the radius of the wire). To remove this gap, the residual stresses were reconstructed on the basis of the indicated limited data of X-ray measurements [5] for the stress σ_{zR} in the wires under consideration. We restricted our analysis to the axisymmetric problem in cylindrical coordinates (r, θ, z) and estimated the hoop residual stress $\sigma_{\theta R}(r)$ for the depths where the measurements were performed according to the available distributions of axial residual stresses $\sigma_{zR}(r)$ by using a similitude hypotheses derived from the analysis of the more representative sets of measurements of both σ_{zR} and $\sigma_{\theta R}$ in similar cases [4, 5]. Then, for greater depths (down to the axis of the wire), all distributions of stresses were extrapolated by quadratic parabolas satisfying the global equilibrium conditions over the respective transverse and axial cross sections of a wire. The radial stress $\sigma_{rR}(r)$ was evaluated afterward from the reconstructed distribution of $\sigma_{\theta R}(r)$ according to the standard equilibrium equation of the axisymmetric problem of solid mechanics reduced, in our case, to the following problem:

$$\frac{d(r\sigma_{rR})}{dr} = \sigma_{\theta R}. \tag{7}$$

The hydrostatic residual stresses

$$\sigma_R = \frac{\sigma_{rR} + \sigma_{\theta R} + \sigma_{zR}}{3}$$

obtained according to this procedure are presented in Fig. 1. It is seen that the rolling process introduces severe inhomogeneity of residual stresses (samples C8 and C26) in contrast to relatively more uniform distributions obtained after drawing without rolling (samples C0).

These nonuniform residual stresses appear as a consequence of the inhomogeneous near-surface plastic deformation due to rolling. The variation of the width of X-ray diffraction peak was suggested as an indicator of the inhomogeneity of plastic strains [5]. According to the reported measurements [5], the distribution of plastic strains after cold drawing without rolling is relatively homogeneous. By using the condition of plastic incompressibility and the reduction of the diameter of the rod by cold drawing, the corresponding background level of equivalent plastic strains in wires after drawing can be estimated as $\varepsilon_{p0} = 2\ln(d/d_0)$. Then, for the wires C8 and C26 subjected to rolling, the equivalent distributions of plastic strains affected by this treatment can be approximated by using the corresponding X-ray data [5] in a rough piecewise-linear manner, as shown in Fig. 1.

Model of Hydrogen-Induced Fracture. As for fracture, the adopted model is basically identical to the model proposed and substantiated in the previous work [6]. Thus, HIF is regarded as a stress-controlled phenomenon. Hence, for wires under consideration, the general-form criterion of HIF (2) is specialized and states that fracture is initiated (and a surface crack of depth x_c is assumed to appear) if the average hydrogen concentration

$$\langle C(r,t)\rangle_{x_c} = \frac{1}{x_c}\int_{a-x_c}^{a} C(r,t)\,dr \tag{8}$$

attains the level $C_{\rm cr}(\langle\sigma_{z,\rm ef}\rangle_{x_c})$ over a critical initiation scale x_c; here, the effective crack opening stress $\sigma_{z,\rm ef}$ is the sum of the applied and residual axial stresses, i.e., $\sigma_{z,\rm ef} = \sigma_{ap} + \sigma_{zR}$, and its average value $\langle\sigma_{z,\rm ef}\rangle_{x_c}$ over the same scale x_c is defined by analogy with the averaging procedure specified by relation (8). The phase of subcritical crack growth from the size x_c to terminal rupture is neglected. For high-strength wires, it was shown that this assumption is in reasonably good agreement with the experiments [6]. Therefore, the fracture condition is expressed in terms of the critical value of the stress intensity factor $K_{\rm I}$:

$$K_{\rm I}(x_c, \sigma_{z,\rm ef}) = K_{\rm IHAC}, \tag{9}$$

where $K_{\rm IHAC}$ is the critical stress intensity factor for hydrogen-assisted cracking under given environmental conditions.

It is assumed that the role of fracture embryo is played by a surface semielliptic crack with depth-to-width aspect ratio equal to 0.2 (this is substantiated in [6]). For any $\sigma_{z,\rm ef}(r)$, the values of the stress intensity factor can be found by the method of weight functions [11]. However, for all considered distributions of $\sigma_{zR}(r)$ which turn out to be quite similar in the analyzed case to the $\sigma_R(r)$-paths depicted in Fig. 1 for the relevant range of crack depths, it is shown that the values of $K_{\rm I}$ can be found with an error lower than 5% by the formula [6]:

$$K_{\rm I} = 0.94\,\langle\sigma_{z,\rm ef}\rangle_{x_c}\sqrt{\pi x_c}\,. \tag{10}$$

Then, the critical scale for HIF is found from Eqs. (9) and (10):

$$x_c = \frac{1}{\pi}\left(\frac{K_{\mathrm{IHAC}}}{0.94\langle\sigma_{z,\mathrm{ef}}\rangle_{x_c}}\right)^2. \tag{11}$$

Finally, if x_c is determined, then the specific criterion for HIF in prestressing steel wires under consideration can be established as a result of averaging of the relation (2) over the fracture scale x_c by analogy with relation (8). Hence, the equation used to predict the life of wire t_f takes the form:

$$\langle C(r, t_f)\rangle_{x_c} = C_{\mathrm{cr}}(\langle\sigma_{z,\mathrm{ef}}\rangle_{x_c}). \tag{12}$$

This allows us to find t_f on the basis of the solution $C(r, t)$ of the problem (4)–(6) of stress–strain assisted diffusion of hydrogen in a loaded wire during the ATT.

Life Prediction for Wires

The model presented in the previous section makes it possible to elucidate the role of residual stress-strain profiles (and respective surface treatments) in the HIF of wires and predict their time to fracture in hydrogenating environments. To apply the model to the analysis of ATT [5, 6], a set of material properties must be specified. According to the available experimental knowledge, the input data were chosen as follows:

The temperature was fixed to be $T = 323°\mathrm{K}$. The partial molar volume of hydrogen in steels is known to be practically constant: $V_H = 2\,\mathrm{cm}^3/\mathrm{mole}$ [6, 10]. As for the diffusion coefficient, the measured data are, as a rule, characterized by a significant dispersion at ambient temperatures for nominally the same alloys, the data on hydrogen solubility are also fairly ambiguous, and all these data are very sensitive to fine peculiarities of the composition of alloy and its microstructure [10, 12]. The quantitative information about their dependence on plastic strains is poor for most commercial alloys. Nevertheless, for the analyzed range of ε_p, the following data were suggested as reasonable estimations [6, 12, 13]:

$$D(\varepsilon_p) = D_0 \exp(-\alpha\varepsilon_p) \quad \text{with} \quad \alpha = 2.9, \tag{13}$$

$$K_{S\varepsilon}(\varepsilon_p) = 1 + \beta\varepsilon_p \quad \text{with} \quad \beta = 4, \tag{14}$$

where D_0 is the diffusion coefficient in strain-free steel rod (in the as-received state, i.e., prior to cold drawing); $D_0 = 3\cdot 10^{-12}\,\mathrm{m}^2/\mathrm{sec}$ at the indicated temperature. Finally, $K_{\mathrm{IHAC}} = 0.27\,K_{IC}$ for the commercial prestressing steel in the ATT solution [6].

To evaluate the left-hand side of equation (12), the evolution of hydrogen concentration in the samples can be determined in terms of the dimensionless concentration $C(r, t)/C_\Gamma$ as a result of the solution of the problem of stress-strain-assisted diffusion (4)–(6). (It is worth noting that, according to relation (6), the concentration C_Γ is a function of stresses and strains.) Here, we use the trivial initial conditions, i.e., $C(r, 0) = 0$.

The numerical analysis of axisymmetric stress-strain-affected diffusion was carried out as described in [14, 15] following the standard weighted residual process to construct a finite-element approximation of the initial-boundary-value problem (4)–(6).

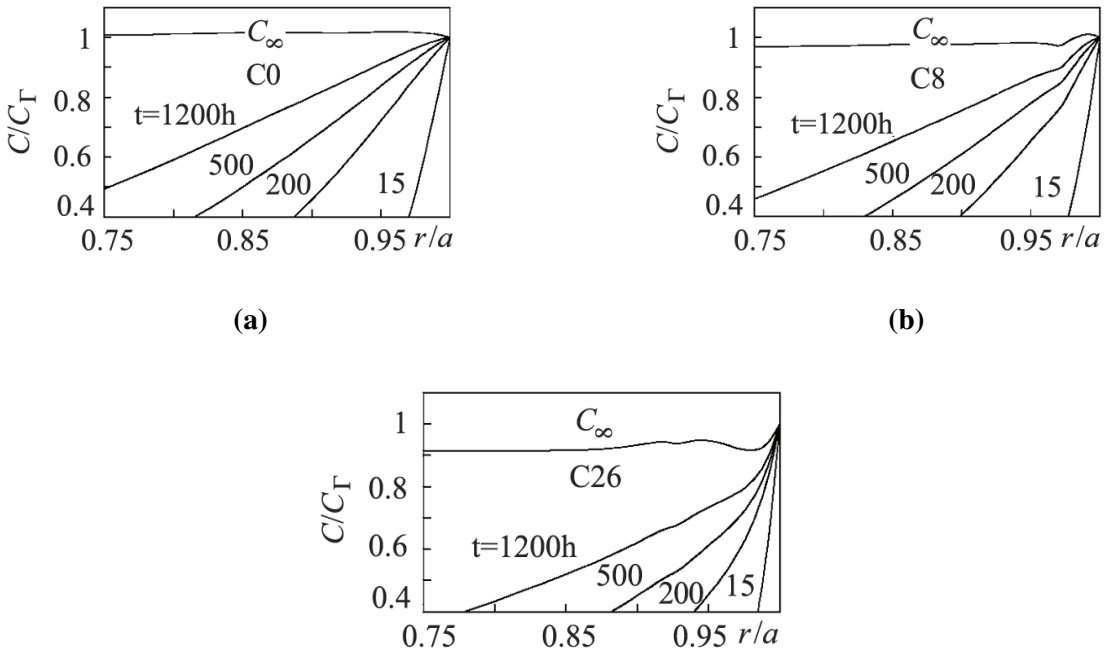

Fig. 2. Results of the numerical analysis of stress-strain-assisted diffusion for residual stress and plastic strain distributions in the C0 (a), C8 (6) and C26 (c) wires for various (indicated) periods of diffusion (hours).

In brief, we applied the Galerkin process to the continuum discretized into finite elements with the same shape functions $\{W_m(r);\ m = 1, 2, \ldots, M\}$, where M is the number of nodes of the mesh, served as trial and weighting functions, and also used to approximate the stress distributions $\sigma(r)$, the diffusion coefficient (13) and solubility (14) depending on the plastic strain $\varepsilon_p(r)$. Then the weak form of the weighted residual statement of the problem rendered a system of ordinary differential equations with respect to time for the nodal values of the concentration C. To solve this system, we used the unconditionally stable Galerkin scheme of time-domain integration. Simulations were performed by using linear trial functions. Nonuniform space discretization was employed to fit the steep gradients of stresses (see Fig. 1) and concentration. The smallest finite elements were about $5\ \mu$m in length.

For all three profiles of the residual stress–strain field in wires shown in Fig. 1, the dimensionless results of computations of the diffusion process are presented in Fig. 2 together with the corresponding equilibrium distributions of concentration as $t \to \infty$ given by the known steady-state solution of the problem $C_\infty(r) = C_e K_S(\sigma(r), \varepsilon_p(\Gamma))$ [7–9]. The effect of the rolling-induced stress–strain field is noticeable mostly in the near-surface zone, where the interaction of stress- and strain-controlled solubility terms [cf. Eqs. (3), (13), and (14) and Fig. 1] causes respective concentration peaks. A slight delay of hydrogenation is observed, which increases with more intense rolling, in part due to the local decrease in diffusivity $D(\varepsilon_p)$ at elevated intensities of plastic strains ε_p (i.e., the density of traps; cf. Eq. (13) and Fig. 1).

To give theoretical predictions of the lives of wires in terms of the plots of applied stress vs. time to fracture, the values of $C_{\rm cr}$ for respective wires were calculated according to the presented HIF model after diffusion simulations as the average values (8) of the obtained solutions $C(r, t)$ for the experimentally determined times to fracture in the ATT solution of all three wires at a certain single load level, namely, for the values of $t = t_f$ available for all three wires at the same load level $\sigma_{ap} = 1346$ MPa [5], as shown by the squares in Fig. 3.

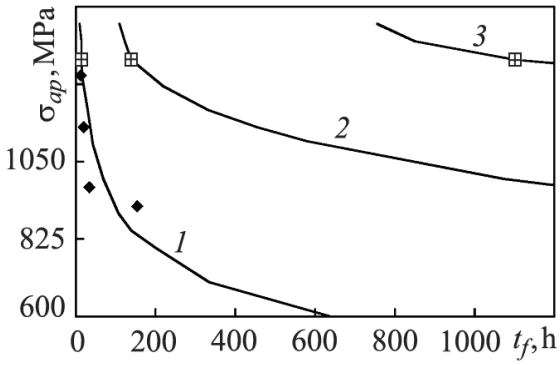

Fig. 3. Theoretical predictions of the lives of prestressing steel wires t_f vs. the applied stress σ_{ap} in the ATT solution for C0 (1), C8 (2) and C26 (3) samples and the respective source data of single experiments (squares) [5]; the dark rhombi mark the experimental data for a steel similar to C0 [6].

Then the entire $\sigma_{ap}(t_f)$-curves were reconstructed as a result of the solution of Eq. (12) by using the results of the diffusion calculations together with the values of C_{cr} estimated according to the data of the mentioned experiments, which were regarded as constants for the respective wires C0, C8, and C26 in a relatively narrow range of the applied stresses under consideration. These curves are displayed in Fig. 3. The experimental data [6] obtained for various load levels for a steel nominally identical to C0 but from a different commercial stock are also shown in Fig. 3.

The agreement between the model predictions and the experimental results is satisfactory and, hence, the presented HIF model seems to be able to give reasonable predictions of the life of prestressing steel under the conditions of hydrogen embrittlement with regard for the role of residual stress profiles induced by the processes of surface treatment. The model provides a tool to analyze and explain their effect by the influence on the stress-and-strain-assisted diffusion of hydrogen toward the rupture sites.

The presented theory can be used, in particular, to reduce the terms and costs of the experiments aimed at the evaluation of the susceptibility of wires to hydrogen embrittlement by performing only limited short-term tests at elevated load levels, estimating the critical concentration C_{cr} according to the data of these tests, and then reconstructing the entire $\sigma_{ap}-t_f$ curves as described earlier. These theoretical curves must give safe (lower-bound) estimations of the life for lower load levels. This is true because, for lower σ_{ap}, the actual critical concentrations can be only higher than the value of C_{cr} theoretically estimated according to the elevated-load data and, hence, the actual time of hydrogenation required to reach the critical condition must be longer than the theoretical prediction. Obviously, the adequate estimation of the diffusion coefficient D is crucial for the quantitative reliability of these predictions in absolute values, although this does not affect the evaluation (prediction) of the consequences of surface treatments in relative terms.

CONCLUSIONS

A model based on the theory of stress-and-strain-assisted diffusion of hydrogen in metals and on the stress-based criterion of hydrogen-assisted local fracture was developed to predict the lives of high-strength steel wires under the conditions promoting hydrogen-induced fracture (HIF).

The realistic residual stress and plastic strain profiles in the prestressing steels subjected to various surface treatments were reconstructed on the basis of the data of limited X-ray diffraction measurements and their effects on the HIF susceptibility were calculated according to the proposed model. Satisfactory agreement was obtained with the available experimental data concerning the time to failure in standard FIP tests.

The proposed computational model seems to be a promising tool for the prediction of the lives of prestressing steel wires under the conditions of HIF on the basis of the data of reduced testing and for the analysis of the influence of various residual stress and strain profiles induced by surface treatments.

Acknowledgements. The financial support of the present work by the Spanish MCYT (Grant MAT2002-01831), Junta de Castilla y León (Grants SA078/04 and SA067A05), as well as by the UE/FEDER (Project RTCT-B-Z/SP.2P18) is gratefully acknowledged. One of the authors (V.Kh.) is indebted for the sponsorship to the Materials Science Group of the University of Salamanca.

REFERENCES

1. A. Valiente and M. Elices, "Premature failure of prestressed steel bars," *Eng. Fail. Anal.,* **5**, 219–227 (1998).
2. F. Bergsma, J. W. Boon, and C. F. Etienne, "Détermination de la sensibilité des aciers précontrains à la fragilisation par l'hydrogène," *Rev. Métalurg.,* **75**, 153–164 (1978).
3. FIP-78. *Stress Corrosion Test. Stress Corrosion Cracking Resistance for Prestressing Tendons,* Techn. Rep. No. 5, FIP, Wexham Springs (Slough, UK) (1981).
4. E. Macherauch, "Introduction to residual stress, " in: *Advances in Surface Treatment,* Vol. 4, Oxford (1987), pp. 1–36.
5. J. M. Campos and M. Elices, "Tensiones residuales internas en alambres trefilados," *Anal. Mecán. Fract.,* **4**, 143–157 (1987).
6. J. Toribio and M. Elices, "Influence of residual stresses on hydrogen embrittlement susceptibility of prestressing steels," *Int. J. Sol. Struct.,* **28**, 791–803 (1991).
7. J. Toribio and V. Kharin, "*K*-dominance condition in hydrogen assisted cracking: the role of the far field," *Fatigue Fract. Eng. Mater. Struct.,* **20**, 729–745 (1997).
8. J. Toribio and V. Kharin, "Evaluation of hydrogen assisted cracking: the meaning and significance of the fracture mechanics approach," *Nucl. Eng. Design,* **182**, 149–163 (1998).
9. J. Toribio and V. Kharin, "The effect of history on hydrogen assisted cracking: 1. Coupling of hydrogenation and crack growth," *Int. J. Fract.,* **88**, 233–245 (1998).
10. J. P. Hirth, "Effects of hydrogen on the properties of iron and steel," *Metal. Trans.,* **11A**, 861–890 (1980).
11. T. Fett and D. Munz, *Stress Intensity Factors and Weight Functions,* Computational Mechanics Publications, Southampton–Boston (1997).
12. F. R. Coe and J. Moreton, "Diffusion of hydrogen in low-alloy steel," *J. Iron Steel Inst.,* **204**, 366–370 (1966).
13. M. A. Astiz, J. A. Áfvarez, and F. Guitiérrez-Solana, "Modelo numérico para analizar el efecto del hidrógeno sobre los procesos de fisuración dúctil," *Anal. Mecan. Fract.,* **15**, 79–84 (1998).
14. J. Toribio and V. Kharin, "Role of fatigue crack closure stresses in hydrogen assisted cracking," in: *Advances in Fatigue Crack Closure Measurement and Analysis,* Vol. 2, ASTM STP 1343, ASTM, Philadelphia (1999). pp. 440-445.
15. J. Toribio and V. Kharin, "Influence of cyclic preloading on hydrogen degradation of materials," *Fiz.-Khim. Mekh. Mater.,* **38**, No. 4, 43–52 (2002).